Published in final edited form as:

Mol Neurobiol. 2019 April ; 56(4): 2353–2361. doi:10.1007/s12035-018-1228-0.

IVIG Delays Onset in a Mouse Model of Gerstmann-Sträussler-Scheinker Disease

Huiying Gu[1], **Yvonne Kirchhein**[1,2], **Timothy Zhu**[1], **Gang Zhao**[1,3], **Hongjun Peng**[4], **Eileen Du**[5], **Junyi Liu**[6], **James A. Mastrianni**[7], **Martin R. Farlow**[1], **Richard Dodel**[2], and **Yansheng Du**[1,8]

[1]Department of Neurology, Indiana University School of Medicine, Indianapolis, IN 46202, USA

[2]Department of Neurology, Philipps-University Marburg, Marburg, Germany

[3]School of Basic Medical Sciences, Hubei University of Chinese Medicine, Wuhan, People's Republic of China

[4]Department of Pediatrics, Jinling Hospital, Nanjing University School of Medicine, Nanjing 210002, China

[5]Department of Psychology, Boston College, Chestnut Hill, MA 02467, USA

[6]Department of Chemical Biology, School of Pharmaceutical Sciences, Peking University, Beijing 100191, China

[7]Department of Neurology, University of Chicago, Chicago, IL 60637, USA

[8]Department of Anatomy and Histology, School of Basic Medical Sciences, Tianjin Medical University, Tianjin 300070, China

Abstract

Our previous studies showed that intravenous immunoglobulin (IVIG) contained anti-Aβ autoantibodies that might be able to treat Alzheimer's disease (AD). Recently, we identified and characterized naturally occurring autoantibodies against PrP from IVIG. Although autoantibodies in IVIG blocked PrP fibril formation and PrP neurotoxicity in vitro, it remained unknown whether IVIG could reduce amyloid plaque pathology in vivo and be used to effectively treat animals with prion diseases. In this study, we used Gerstmann-Sträussler-Scheinker (GSS)-Tg (PrP-A116V) transgenic mice to test IVIG efficacy since amyloid plaque formation played an important role in GSS pathogenesis. Here, we provided strong evidence that demonstrates how IVIG could significantly delay disease onset, elongate survival, and improve clinical phenotype in Tg (PrP-A116V) mice. Additionally, in treated animals, IVIG could markedly inhibit PrP amyloid plaque formation and attenuate neuronal apoptosis at the age of 120 days in mice. Our results indicate that IVIG may be a potential, effective therapeutic treatment for GSS and other prion diseases.

Yansheng Du, ydu@iupui.edu.

Authors' Contribution HG prepared figures and wrote the main manuscript text. YK, TZ, GZ, and HP prepared figures. JM provided the study materials. JL, MF, and RD designed experiments and performed admin-istrative support. ED collected and analyzed data and revised the manuscript. YD designed experiments, performed financial support, and did the final approval of the manuscript. All authors reviewed the manuscript.

Competing Interests The authors declare that they have no competing interests.

Keywords

Prion; IVIG; Amyloid plaque; Apoptosis

Introduction

Prion diseases, also known as transmissible spongiform en-cephalopathies (TSEs), are a group of rare progressive neurodegenerative disorders linked to the accumulation of misfolded, self-replicating, and proteinase K-resistant conformers, termed scrapie PrP (PrP^{Sc}) from the normal cellular prion protein (PrP^{C}) [1]. They are characterized by spongiform degeneration of the central nervous system (CNS) consisting of neuronal death, insoluble prion amyloid aggregates, astrogliosis, and neuroinflammation [2]. TSEs caused by altered forms of PrP include scrapie in sheep and bovine spongiform encephalopathy in cattle, as well as the human forms Kuru, Creutzfeldt-Jakob disease (CJD and vCJD), and the Gerstmann-Sträussler-Scheinker (GSS) syndrome [3]. GSS is an inherited prion disease, typified by the onset of progressive ataxia (incoordination), the progression of dementia, and the presence of PrP amyloid deposits forming plaques in the brain. Recently, a GSS-Tg (PrP-A116V) transgenic mouse model was established and characterized [4].

The PrP^{Sc} aggregates in affected brain areas are thought to lead to neuronal dysfunction and neuronal death, which leads to clinical symptoms [3, 5, 6]. PrP^{Sc} represents a primary target for therapeutic strategies [7]. The expression of PrP^{C} is not restricted only to the brain but also occurs in peripheral tissues including normal human lymphocytes, monocytes, neutrophils, and lymphoid cells [8–10]. In fact, PrP^{C} expresses about four times more on activated lymphocytes than resting cells, and thus provides a potential reservoir for PrP^{Sc} replication [8]. Studies show that the latent stage of prion disease is characterized by accumulation of PrP^{Sc} in lymphatic organs such as the spleen, tonsils, lymph nodes, or gut before its accumulation in the CNS [11–13]. The spleen is thought to be the site for initial prion accumulation in bovine spongiform encephalopathy [14]. A number of studies show that spleen follicular dendritic cells (FDCs), stromal cells located in primary B cell follicles and germinal centers of lymphoid tissues, are the main site for prion replication [15]. Impaired neuroinvasion was observed in immunodeficient mice that lacked or had a temporary inactivation of FDCs [16–20]. Therefore, immunotherapy that targets peripheral lymphoid system could be effective in treating prion diseases.

Our previous studies indicated that intravenous immunoglobulin (IVIG) contained anti-Aβ autoantibodies or purified autoantibodies against Aβ, which could be used to treat Alzheimer's disease (AD) [21–26]. Recently, we also detected and purified naturally occurring autoantibodies against PrP from IVIG [27]. These autoantibodies are similar to anti-Aβ antibodies [24, 28] that blocked PrP fibril formation and PrP neurotoxicity. Importantly, autoantibodies with complete human sequences are able to overcome the inflammatory side-effects generated by active immunization or humanized monoclonal antibodies during the chronic therapy. It was reported that two humanized antibodies against PrP95–105 might be proapoptotic in the hippocampus [29]. Interestingly enough, prion autoantibodies had a high affinity for PrP^{Sc}, and protected against neurotoxic effects of

PrP^{Sc} in neuronal cultures [27]. Autoantibodies also enhanced the uptake of PrP106–126 A117V in microglial cells without inducing an inflammatory response [30]. Thus, IVIG and these autoantibodies have a large potential to be quickly and effectively used in clinical studies for prion disease.

While much work has been done with in vitro studies, the effect of IVIG in genetic prion disease and amyloid plaque pathology remains to be unclear. To address these questions, we treated (PrP-A116V) mice with IVIG to investigate whether IVIG could delay disease onset and reduce amyloid plaque formation.

Materials and Methods

Animals and Treatments

The GSS-Tg (PrP-A116V) transgenic mouse model has been described previously [4]. Mice that carry the mouse homolog of the GSS-associated A116V mutation expressed approximately six times the endogenous levels of PrP. Tg (PrP-A116V) mice developed progressive ataxia around 120 days and died at approximately 180 days. In this study, mice were bred in the laboratory of the Animal Center at Indiana University School of Medicine and were housed 3–5 per cage, fed with food and water ad libitum, and maintained in a 12-h light/dark cycle facility. Male and female mice were randomly used and administered with 20 mg/kg IVIG (Bayer, Pittsburgh, PA, USA) [31] via intraperitoneal (IP) injection weekly starting from 90 days after birth until they reached the end of point (20% in body weight loss relative to the onset stage) or the indicated experimental time. Control mice received the same volume of PBS without IVIG. All animal procedures were performed in accordance with the protocols approved and authorized by the Institutional Animal Care and Use Committee at Indiana University School of Medicine.

Clinical Assessment

At the start of the treatment, mice were monitored daily for signs of prion disease, including gait ataxia, hunched posture, and poor righting reflex. A detailed clinical assessment scale to monitor the progression of disease was developed. Ataxia and mobility problems are key features of this mouse model and were heavily weighted in the assessment. The following score from 0 to 5 was used: 0 = no ataxia; 1 = no ataxia, but may show other signs such as walking lower to the ground; 2 = more consistent, but still with a subtle change in gait (wider, lower to ground), but not definitive ataxia; 3 = persistent and obvious wobble—this stage defined the clear onset of ataxia; 4 = stumble/loss of footing (mouse might occasionally start to sway (rock back and forth) when in a stationary position) and obvious weight loss; 5 = lethargic, very hunched, and emaciated. Mice were generally killed during stage 4 or 5 as they could no longer be fed, and there was a 20% in body weight loss relative to the onset stage. Ataxia typically developed around 120 days of age.

Histology and Immunohistochemistry

Paraffin Sections—Mice were euthanized with CO_2 and slowly perfused via cardiac puncture with 20 ml of phosphate buffered saline (PBS) followed by 20 ml of 4% paraformaldehyde (PFA, Sigma-Aldrich, St. Louis, MO, USA). Brains were stored in 4%

PFA for 48 h and then transferred to PBS containing 0.1% sodium azide (Sigma-Aldrich, St. Louis, MO, USA). Brains were embedded in paraffin for cutting sections. The blocks of mouse cerebella were cut at similar landmarks of the cerebellum into 10-μm coronal sections. Paraffin slides were deparaffinized in xylene (Thermo Fisher Scientific, Waltham, MA, USA) and rehydrated using graded percentages of ethanol immediately before staining [32, 33].

Thioflavin S Staining—Sections were stained with 0.05% thioflavin S (Sigma-Aldrich, St. Louis, MO, USA) for detection of PrP amyloid plaque deposits and with 6-diamidino-2-phenyl-indole, dihydrochloride (DAPI, Vector, Burlingame, CA, USA) to visualize nuclei. Slides were observed using a fluorescence microscope. Positive plaques were counted in nine sections (spaced 210 μm apart) from each cerebellum. The total surface area of plaque deposit was measured using ImageJ and expressed as a percentage of the total surface of the cerebellum.

Terminal Deoxynucleotidyl Transferase-Mediated Biotinylated UTP Nick End Labeling—DNA fragmentation was assessed with terminal deoxynucleotidyl transferase-mediated biotinylated UTP nick end labeling (TUNEL) apoptosis detection kit (MilliporeSigma, Burlington, MA, USA), following the manufacturer's instruction. Briefly, sections were incubated with proteinase K for 30 min at 37 °C. After incubation with a reaction mixture containing biotin-dUTP and terminal deoxynucleotidyl transferase (TdT) for 60 min, sections were incubated with avidin–FITC solution for 30 min at 37 °C in the dark. The fixed sections were incubated with 5 μg/ml DNase I for 60 min at 37 °C before labeling as positive control. For nuclear staining, air dried sections were mounted with mounting medium with DAPI. Sections were observed under a fluorescence microscope. The apoptosis was determined by percentage area of TUNEL-positive signal relative to the area of DAPI stain in each cerebellar section using ImageJ [32, 34].

Immunofluorescence of NeuN—Brain sections were first TUNEL stained with the proteinase K step eliminated blocked with 2% BSA in PBS for 1 h, and then incubated with rabbit anti-NeuN antibody (1500) (MilliporeSigma, Burlington, MA, USA) overnight. Alexa Fluor 647 chicken anti-rabbit IgG (H+L) (Life Technologies, Grand Island, NY, USA) was used as secondary antibody. Results were visualized by a fluorescence microscopy.

Immunofluorescence of GFAP and Iba1—Brain sections were incubated with rabbit anti-ionized calcium-binding adapter molecule 1 antibody (1:2000, Abcam, Cambridge, MA, USA) or mouse anti-glia fibrillary acidic protein (GFAP, 1:1000, MilliporeSigma, Burlington, MA, USA) followed by an alexa fluo 488 anti-rabbit or mouse IgG (Invitrogen, Carlsbad, CA, USA). Results were visualized under the fluorescence microscope [33].

Statistical Analysis

Statistical analyses of the differences between groups were carried out by a one-way ANOVA with post hoc comparisons by Dunnett's test. All data are expressed as mean ± SD. Differences between two means were considered significant when p was equal or less than 0.05.

Results

IVIG Delayed Disease Onset and Improves Clinical Phenotype of TG (PrP-A116V) Mice

TG (PrP-A116V) exhibited normal behavior and activity before disease onset. They began to display early signs of gait ataxia, the primary manifestation of GSS, around 4 months old. Mice around 60 days after birth showed higher levels of disability and lower survival rate [4].

We developed a scale scoring system that ranges from 0 (no disease) to 5 (terminal) to investigate the effect of IVIG on the disease onset, progression, and duration. The disease onset was defined as score 3, when ataxia was persistent and obviously present (see "Materials and Methods" for details of the ataxia assessment). Mice were generally killed during stage 4 or 5, as they could no longer be fed, and there was a 20% body weight loss from the onset stage. The mean age at disease onset of vehicle-treated control mice was 116.9 ± 5.1 days (Fig. 1a). There was minimal difference between controls and untreated TG (PrP-A116V) mice (data not shown), suggesting that the stress of injection and handling did not affect disease onset. The mean age of onset was 130.2 ± 7.6 days in 20 mg/kg IVIG-treated mice, which is a significant delay (11.4%) as compared to the onset of control mice ($p < 0.05$).

To assess the effect of IVIG on disease progression of Tg (PrP-A116V) mice, we calculated the average disability score of mice beginning at 100 days until 190 days when the majority of vehicle-treated mice were dead. A significant improvement in disability score was present at most time points, indicating that IVIG shifted the disability curve to the right (Fig. 1b). This data was also presented as bar graphs that displayed the percentage of mice within each clinical disability stage at each time point (Fig. 1c–d). Throughout the observation period, IVIG-treated mice showed lower disability scores as compared to control mice (Fig. 2c–d).

IVIG Elongated Survival of Tg (PrP-A116V) Mice

Tg (PrP-A116V) mice were euthanized at the terminal clinical stage of disease (end of stage 4, beginning of stage 5) when mice became severely disabled and more than 20% of its body weight was lost. To determine whether IVIG delayed death in Tg (PrP-A116V) mice, survival time among the IVIG-treated mice and control mice was compared and survival curves for each group were plotted in Fig. 2a. A significant ($p < 0.05$) improvement in survival time was present in mice that received IVIG, indicating that IVIG shifts the survival curve to the right. By comparing the mean age at death of IVIG-treated mice and control mice, a similar relationship was found. IVIG significantly delayed the mean age at death to 191 ± 12.3 days compared to 179 ± 18.2 days for the control group (Fig. 2b).

IVIG Inhibited PrP Amyloid Plaque Formation in Tg (PrP-A116V) Mice at 120 Days of Age

Deposition of thioflavin S-positive PrP amyloid plaques in the cerebellum is the pathognomonic feature of GSS in humans and the most prominent histopathological feature in Tg (PrP-A116V) mice [4]. The mean age at disease onset was 116.9 ± 5.1 days in control and 130.2 ± 7.6 days in IVIG-treated mice. In order to determine whether the IVIG-induced delayed onset was related to the reduction in PrP plaque deposition, we compared the

thioflavin S-positive plaque burden within the cerebellum of mice from both IVIG-treated and control mice at 120 days of age. The area of thioflavin S staining per total area, as a fraction of the total area of the cerebellar section, was determined using ImageJ and plotted as the relative plaque burden by normalizing each group to the control group. In mice receiving IVIG, almost no plaques were detected in sections examined (100 ± 35 vs. 0.1 ± 0.02%, $n = 3$/group, $p < 0.05$, Fig. 3).

We also measured the plaque burden within the cerebella of mice at the terminal stages of disease. Control mice at the terminal stage showed an approximately fivefold increase in the plaque burden, as compared to control mice at 120 days of age (525.5 ± 212.1%). However, as expected, there was no difference in the plaque burden between IVIG-treated mice and control mice at the terminal stage of disease (100 ± 41.1 vs. 99.8 ± 48.9%, $n = 3$/group, Fig. 4).

IVIG Attenuated Neuronal Apoptosis in Tg (PrP-A116V) Mice at 120 Days of Age

IVIG treatment was shown to reduce Aβ-induced neuronal apoptosis [35]. Here, we investigated whether IVIG treatment also reduces neuronal apoptosis in Tg (PrPA116V) mice. Cerebellar tissues were stained with TUNEL and NeuN together to assess neuronal apoptosis. Similar to studies on PrP amyloid deposition, we examined mice at 120 days of age. Interestingly, TUNEL-positive nuclei were almost fully associated with the NeuN-positive nuclei, indicating that the neuronal apoptosis observed in Tg (PrPA116V) mice at 120 days of age occurred mainly in neuronal cells (Fig. 5a). The fraction of apoptotic neurons was also estimated as the TUNEL-positive signal relative to the signal of DAPI-stained nuclei within each cerebellar tissue section. In control mice, the fraction of apoptotic neurons was 0.48 ± 0.20% ($n = 3$) as compared to 0.11 ± 0.02% ($n = 3$) in IVIG-treated mice (Fig. 5b, c), suggesting that IVIG significantly reduced neuronal apoptosis in Tg (PrPA116V) mice at 120 days of age. Consistent to amyloid deposition data, at the terminal stage of disease, neuronal apoptosis was increased to 0.72 ± 0.18% in control mice as compared to 0.66 ± 0.13% in IVIG-treated mice, suggesting IVIG did not affect neuronal apoptosis at late stage of disease (Fig. 5d).

IVIG Did Not Affect Glial Activation in Tg (PrP-A116V) Mice

Glial cell activation was also assessed by using immunohistochemical analyses (Fig. 6). There were similar levels of GFAP immunoreactivity between vehicle-treated controls and IVIG treatment mice at terminal stage (Fig. 6a, b). The number of GFAP-positive astrocytes per section was 107.3 ± 47.9 in the vehicle-treated group and 130.4 ± 31.0 in IVIG-treated mice (Fig. 6b). Furthermore, microglia stained with Iba1 was performed in the cerebellar paraffin-embedded sections and no changes in levels of microglial immunoreactivity between vehicle-treated controls and IVIG-treated mice at terminal stage were observed (Fig. 6c, d). The number of Iba1-positive microglial cells per section was 57.4 ± 8.9 in the vehicle-treated group and 62.3 ± 20.1 in IVIG-treated mice (Fig. 6d).

Discussion

IVIG was found to contain antibodies against Aβ peptides [21] and suggested to be beneficial in AD treatments [22]. However, a recent multicenter double-blinded phase III study of 390 subjects, called the Gammaglobulin Alzheimer's Partnership (GAP), did not meet primary endpoints of slowing cognitive and functional decline [36]. Interestingly, results obtained from this study continued to support IVIG's positive safety profile and showed potentially beneficial effects for pre-specified moderate AD and apoE4 carrier subgroups. Hence, the IVIG treatment for AD is still of considerable interest in the field and there remains the opportunity for testing the extent to which optimized doses of IVIG delivered early enough in the AD trajectory might yet prove beneficial for modifying disease progression [37]. In this study, we tested IVIG for the treatment of prion diseases such as GSS since not like Aβ with an unclear role in AD pathogenesis, the PrP^{Sc} aggregates in affected brain areas were thought to directly lead to neuronal dysfunction and neuronal death, which lead to clinical symptoms [3, 5, 6] and prion autoantibodies in IVIG had a high affinity for PrP^{Sc}, and protected against neurotoxic effects of PrP^{Sc} in neuronal cultures [27]. As expected, we showed that chronic treatments of Tg (PrP-A116V) mice with IVIG significantly delayed disease onset (14 days delay, 11%), reduced disability, and improved survival in these mice. These improvements were consistent with the reductions of PrP amyloid plaque deposition in the mouse brain and neuronal apoptosis at disease onset. IVIG induced such effects when it was administered weekly starting at 90 days after birth. Interestingly, although it elongated survival of GSS mice, IVIG did not significantly elongate the survival time post disease onset. This suggests that IVIG might be the one in humans in which affects the latency period for the prionrelated disease because people can usually develop prion disease up to 30 years after first being exposed to it. In this study, the neuroprotective effect induced by peripherally injected IVIG was modest due to its poor penetration ability through the blood-brain barrier (BBB) [34]. It was quite possible that IVIG could markedly suppress prion replication and infectivity in the peripheral immune system such as the spleen to slow disease onset; however, because IVIG had limited levels of accumulation in the brain, brain prion replication and infectivity could not be inhibited so disease pathogenesis eventually initiated. Our findings may also explain the data obtained from the immunization studies using the genetic prion model, which showed that only disease onset could be completely stopped by the antibody treatment [38]. Similar to our case, anti-PrP antibodies could only suppress pathogenic events occurring in the peripheral immune system but not in the brain system. Importantly, not like inoculation prion models generated from the exogenous inoculated pathogen, PrP^{Sc}, genetic prion diseases initially resulted from endogenous expression and accumulation of mutant prion in both peripheral and CNS systems. Therefore, peripheral immunotherapies including the IVIG treatment could not be used in genetic prion diseases since after the disease onset, the amount of IVIG in the brain was too low [39] to inhibit further pathological development of PrP^{Sc}. Evidence from our study strongly supports this hypothesis by showing there were no effects on brain amyloid deposition, neuronal apoptosis, and glial activation in IVIG-treated mice at the terminal stage of disease as compared to control mice.

Thus, the key to elongating patients' lives who have genetic prion diseases including GSS would be to determine certain brain levels of IVIG by inhibiting brain prion replication. We believe the efficacy of IVIG against genetic prion diseases can be significantly improved if IVIG is directly administered into the brain. In summary, this study suggested IVIG may be useful to treat sporadic and genetic prion disorders. However, it is necessary to develop a better delivery method for IVIG to largely improve its efficacy in the genetic prion disorders including GSS.

Also, it should be noted that the extent to which endogenous anti-PrP antibodies in IVIG plays a role in delaying GSS disease onset remains unclear since in our unpublished data, after removing anti-PrP antibodies by using the PrP affinity column, we did not find that IVIG-induced protective effects were markedly reduced. Thus, a further study is required to investigate the exact molecular mechanism(s) underlying IVIG-induced protection against PrP^{Sc} toxicity.

Funding

This work was supported by Baudrand Research Foundation.

References

1. McKinley MP, Bolton DC, Prusiner SB (1983) A protease-resistant protein is a structural component of the scrapie prion. Cell 35(1): 57–62 [PubMed: 6414721]
2. Prusiner SB (1998) The prion diseases. Brain Pathol 8(3):499–513 [PubMed: 9669700]
3. Prusiner SB (1991) Molecular biology of prion diseases. Science 252(5012):1515–1522 [PubMed: 1675487]
4. Yang W, Cook J, Rassbach B, Lemus A, DeArmond SJ, Mastrianni JA (2009) A new transgenic mouse model of Gerstmann-Straussler-Scheinker syndrome caused by the A117V mutation of PRNP. J Neurosci 29(32):10072–10080. 10.1523/JNEUROSCI.2542-09.2009 [PubMed: 19675240]
5. Bugiani O, Giaccone G, Piccardo P, Morbin M, Tagliavini F, Ghetti B (2000) Neuropathology of Gerstmann-Straussler-Scheinker disease. Microsc Res Tech 50(1):10–15. 10.1002/1097-0029(20000701)50:1<10::AID-JEMT3>3.0.CO;2-6 [PubMed: 10871543]
6. Ghetti B, Piccardo P, Frangione B, Bugiani O, Giaccone G, Young K, Prelli F, Farlow MR et al. (1996) Prion protein amyloidosis. Brain Pathol 6(2):127–145 [PubMed: 8737929]
7. Aguzzi A, Heikenwalder M (2006) Pathogenesis of prion diseases: current status and future outlook. Nat Rev Microbiol 4(10):765–775. 10.1038/nrmicro1492 [PubMed: 16980938]
8. Cashman NR, Loertscher R, Nalbantoglu J, Shaw I, Kascsak RJ, Bolton DC, Bendheim PE (1990) Cellular isoform of the scrapie agent protein participates in lymphocyte activation. Cell 61(1):185–192 [PubMed: 1969332]
9. Meiner Z, Halimi M, Polakiewicz RD, Prusiner SB, Gabizon R (1992) Presence of prion protein in peripheral tissues of Libyan Jews with Creutzfeldt-Jakob disease. Neurology 42(7):1355–1360 [PubMed: 1352391]
10. Bessos H, Drummond O, Prowse C, Turner M, MacGregor I (2001) The release of prion protein from platelets during storage of apheresis platelets. Transfusion 41(1):61–66 [PubMed: 11161247]
11. Heppner FL, Christ AD, Klein MA, Prinz M, Fried M, Kraehenbuhl JP, Aguzzi A (2001) Transepithelial prion transport by M cells. Nat Med 7(9):976–977. 10.1038/nm0901-976 [PubMed: 11533681]
12. Aguzzi A, Sigurdson CJ (2004) Antiprion immunotherapy: to suppress or to stimulate? Nat Rev Immunol 4(9):725–736. 10.1038/nri1437 [PubMed: 15343371]
13. Wisniewski T, Sigurdsson EM (2007) Therapeutic approaches for prion and Alzheimer's diseases. FEBS J 274(15):3784–3798. 10.1111/j.1742-4658.2007.05919.x [PubMed: 17617224]

14. Daude N (2004) Prion diseases and the spleen. Viral Immunol 17(3):334–349. 10.1089/0882824041857139 [PubMed: 15357900]
15. Park CS, Choi YS (2005) How do follicular dendritic cells interact intimately with B cells in the germinal centre? Immunology 114(1): 2–10. 10.1111/j.1365-2567.2004.02075.x [PubMed: 15606789]
16. Glaysher BR, Mabbott NA (2007) Role of the GALT in scrapie agent neuroinvasion from the intestine. J Immunol 178(6):3757–3766 [PubMed: 17339474]
17. Mabbott NA, Williams A, Farquhar CF, Pasparakis M, Kollias G, Bruce ME (2000) Tumor necrosis factor alpha-deficient, but not interleukin-6-deficient, mice resist peripheral infection with scrapie. J Virol 74(7):3338–3344 [PubMed: 10708451]
18. Prinz M, Montrasio F, Klein MA, Schwarz P, Priller J, Odermatt B, Pfeffer K, Aguzzi A (2002) Lymph nodal prion replication and neuroinvasion in mice devoid of follicular dendritic cells. Proc Natl Acad Sci U S A 99(2):919–924. 10.1073/pnas.022626399 [PubMed: 11792852]
19. Montrasio F, Frigg R, Glatzel M, Klein MA, Mackay F, Aguzzi A, Weissmann C (2000) Impaired prion replication in spleens of mice lacking functional follicular dendritic cells. Science 288(5469): 1257–1259 [PubMed: 10818004]
20. Mabbott NA, Mackay F, Minns F, Bruce ME (2000) Temporary inactivation of follicular dendritic cells delays neuroinvasion of scrapie. Nat Med 6(7):719–720. 10.1038/77401 [PubMed: 10888894]
21. Du Y, Dodel R, Hampel H, Buerger K, Lin S, Eastwood B, Bales K, Gao F et al. (2001) Reduced levels of amyloid beta-peptide antibody in Alzheimer disease. Neurology 57(5):801–805 [PubMed: 11552007]
22. Dodel R, Hampel H, Depboylu C, Lin S, Gao F, Schock S, Jackel S, Wei X et al. (2002) Human antibodies against amyloid beta peptide: a potential treatment for Alzheimer's disease. Ann Neurol 52(2): 253–256. 10.1002/ana.10253 [PubMed: 12210803]
23. Dodel RC, Du Y, Depboylu C, Hampel H, Frolich L, Haag A, Hemmeter U, Paulsen S et al. (2004) Intravenous immunoglobulins containing antibodies against beta-amyloid for the treatment of Alzheimer's disease. J Neurol Neurosurg Psychiatry 75(10):1472–1474. 10.1136/jnnp.2003.033399 [PubMed: 15377700]
24. Du Y, Wei X, Dodel R, Sommer N, Hampel H, Gao F, Ma Z, Zhao L et al. (2003) Human anti-beta-amyloid antibodies block betaamyloid fibril formation and prevent beta-amyloid-induced neurotoxicity. Brain 126(Pt 9):1935–1939. 10.1093/brain/awg191 [PubMed: 12821522]
25. Counts SE, Ray B, Mufson EJ, Perez SE, He B, Lahiri DK (2014) Intravenous immunoglobulin (IVIG) treatment exerts antioxidant and neuropreservatory effects in preclinical models of Alzheimer's disease. J Clin Immunol 34(Suppl 1):S80–S85. 10.1007/s10875-014-0020-9 [PubMed: 24760109]
26. Lahiri DK, Ray B (2014) Intravenous immunoglobulin treatment preserves and protects primary rat hippocampal neurons and primary human brain cultures against oxidative insults. Curr Alzheimer Res 11(7):645–654 [PubMed: 25115544]
27. Wei X, Roettger Y, Tan B, He Y, Dodel R, Hampel H, Wei G, Haney J et al. (2012) Human anti-prion antibodies block prion peptide fibril formation and neurotoxicity. J Biol Chem 287(16): 12858–12866. 10.1074/jbc.M111.255836 [PubMed: 22362783]
28. Dodel R, Balakrishnan K, Keyvani K, Deuster O, Neff F, Andrei-Selmer LC, Roskam S, Stuer C et al. (2011) Naturally occurring autoantibodies against beta-amyloid: investigating their role in transgenic animal and in vitro models of Alzheimer's disease. J Neurosci 31(15):5847–5854. 10.1523/JNEUROSCI.4401-10.2011 [PubMed: 21490226]
29. Solforosi L, Criado JR, McGavern DB, Wirz S, Sanchez-Alavez M, Sugama S, DeGiorgio LA, Volpe BT et al. (2004) Cross-linking cellular prion protein triggers neuronal apoptosis in vivo. Science 303(5663):1514–1516. 10.1126/science.1094273 [PubMed: 14752167]
30. Roettger Y, Zerr I, Dodel R, Bach JP (2013) Prion peptide uptake in microglial cells—the effect of naturally occurring autoantibodies against prion protein. PLoS One 8(6):e67743 10.1371/journal.pone.0067743 [PubMed: 23840767]

31. Gu H, Zhong Z, Jiang W, Du E, Dodel R, Farlow MR, Zheng W, Du Y (2014) The role of choroid plexus in IVIG-induced beta-amyloid clearance. Neuroscience 270:168–176. 10.1016/j.neuroscience.2014.04.011 [PubMed: 24747018]
32. Cortes CJ, Qin K, Cook J, Solanki A, Mastrianni JA (2012) Rapamycin delays disease onset and prevents PrP plaque deposition in a mouse model of Gerstmann-Straussler-Scheinker disease. J Neurosci 32(36):12396–12405. 10.1523/JNEUROSCI.6189-11.2012 [PubMed: 22956830]
33. Gu H, Wei X, Monnot AD, Fontanilla CV, Behl M, Farlow MR, Zheng W, Du Y (2011) Lead exposure increases levels of beta-amyloid in the brain and CSF and inhibits LRP1 expression in APP transgenic mice. Neurosci Lett 490(1):16–20. 10.1016/j.neulet.2010.12.017 [PubMed: 21167913]
34. Tan J, Ma Z, Han L, Du R, Zhao L, Wei X, Hou D, Johnstone BH et al. (2005) Caffeic acid phenethyl ester possesses potent cardioprotective effects in a rabbit model of acute myocardial ischemia-reperfusion injury. Am J Phys Heart Circ Phys 289(5): H2265–H2271. 10.1152/ajpheart.01106.2004
35. Widiapradja A, Vegh V, Lok KZ, Manzanero S, Thundyil J, Gelderblom M, Cheng YL, Pavlovski D et al. (2012) Intravenous immunoglobulin protects neurons against amyloid beta-peptide toxicity and ischemic stroke by attenuating multiple cell death path-ways. J Neurochem 122(2):321–332. 10.1111/j.1471-4159.2012.07754.x [PubMed: 22494053]
36. Relkin N (2014) Clinical trials of intravenous immunoglobulin for Alzheimer's disease. J Clin Immunol 34(Suppl 1):S74–S79. 10.1007/s10875-014-0041-4 [PubMed: 24760112]
37. Counts SE, Lahiri DK (2014) Overview of immunotherapy in Alzheimer 's disease (AD) and mechanisms of IVIG neuroprotection in preclinical models of AD. Curr Alzheimer Res 11(7):623–625 [PubMed: 25156573]
38. White AR, Enever P, Tayebi M, Mushens R, Linehan J, Brandner S, Anstee D, Collinge J et al. (2003) Monoclonal antibodies inhibit prion replication and delay the development of prion disease. Nature 422(6927):80–83. 10.1038/nature01457 [PubMed: 12621436]
39. St-Amour I, Bousquet M, Pare I, Drouin-Ouellet J, Cicchetti F, Bazin R, Calon F (2012) Impact of intravenous immunoglobulin on the dopaminergic system and immune response in the acute MPTP mouse model of Parkinson's disease. J Neuroinflammation 9:234 10.1186/1742-2094-9-234 [PubMed: 23046563]

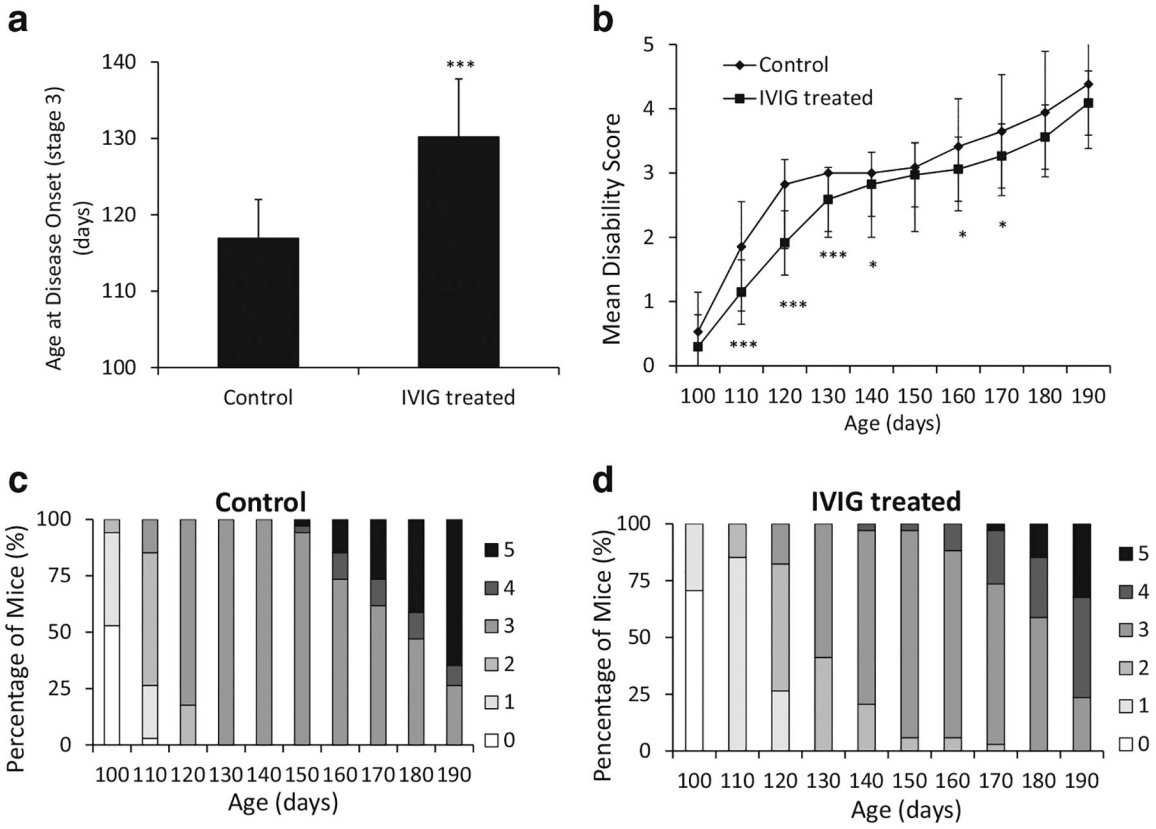

Fig. 1.

IVIG delays disease onset and progression in Tg (PrP-A116V) mice. **a** Age of disease onset (stage 3) of Tg (PrP-A116V) mice treated with PBS or IVIG at 20 mg/kg [31], beginning at 90 days of age. **b** Disability scores of Tg (PrP-A116V) mice plotted over time. Animals were assessed twice weekly and scored according to a disability scale that range from 0 to 5, until they were euthanized. **c** and **d** The bars represent the percentage of Tg (PrP-A116V) mice within each stage of disease at the indicated time point. Data represent mean ± SD, n = 34/group, *$p < 0.05$, ***$p < 0.001$

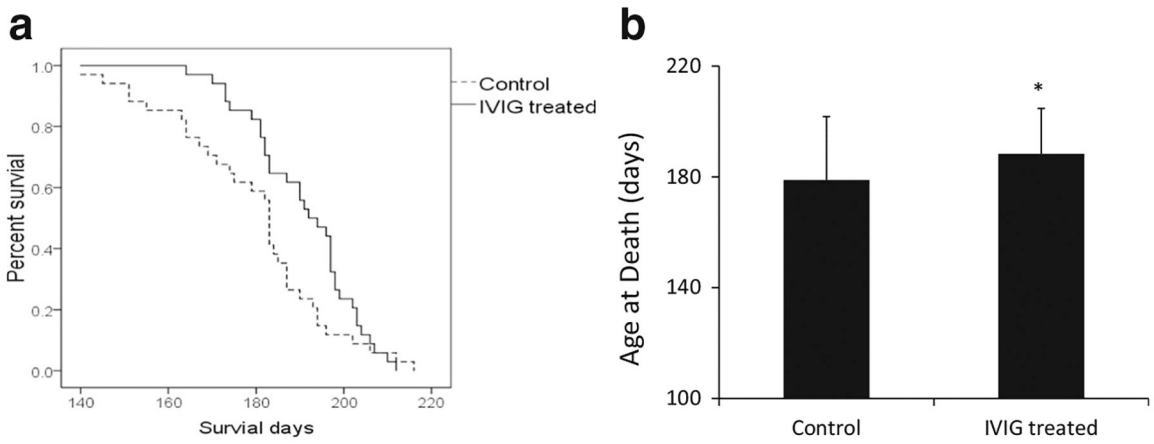

Fig. 2.

IVIG elongates survival of Tg (PrP-A116V) mice. **a** Kaplan-Meier survival curve of mice treated with PBS or IVIG once per week, beginning at 90 days of age. **b** Age at death of Tg (PrP-A116V) mice treated with PBS or IVIG. Data represent mean ± SD, $n = 34$/group, $^*p < 0.05$

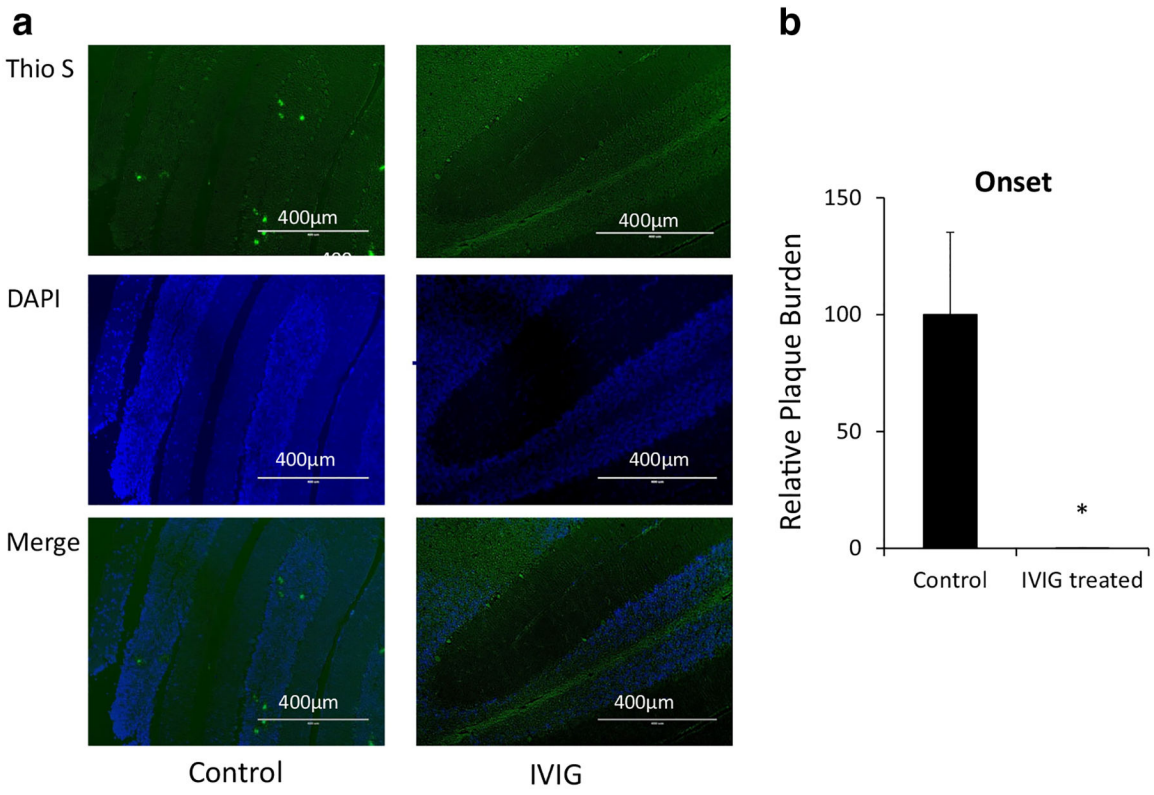

Fig. 3.

IVIG inhibits PrP amyloid plaque deposition in Tg (PrP-A116V) mice at onset stage. **a** Representative cerebellar sections stained with thioflavin S at 120 days old Tg (PrP-A116V) mice (onset stage) treated with PBS (control) or IVIG. **b** Quantification of amyloid load in cerebella: nine coronal sections per cerebellum stained with thioflavin S were used to quantify PrP amyloid plaques. Nuclei were stained with DAPI. All sections were visualized by fluorescence microscopy and data were expressed as the relative plaque burden, by normalizing each group to the control group. Data represent mean ± SD, $n = 3$/group, $*p < 0.05$

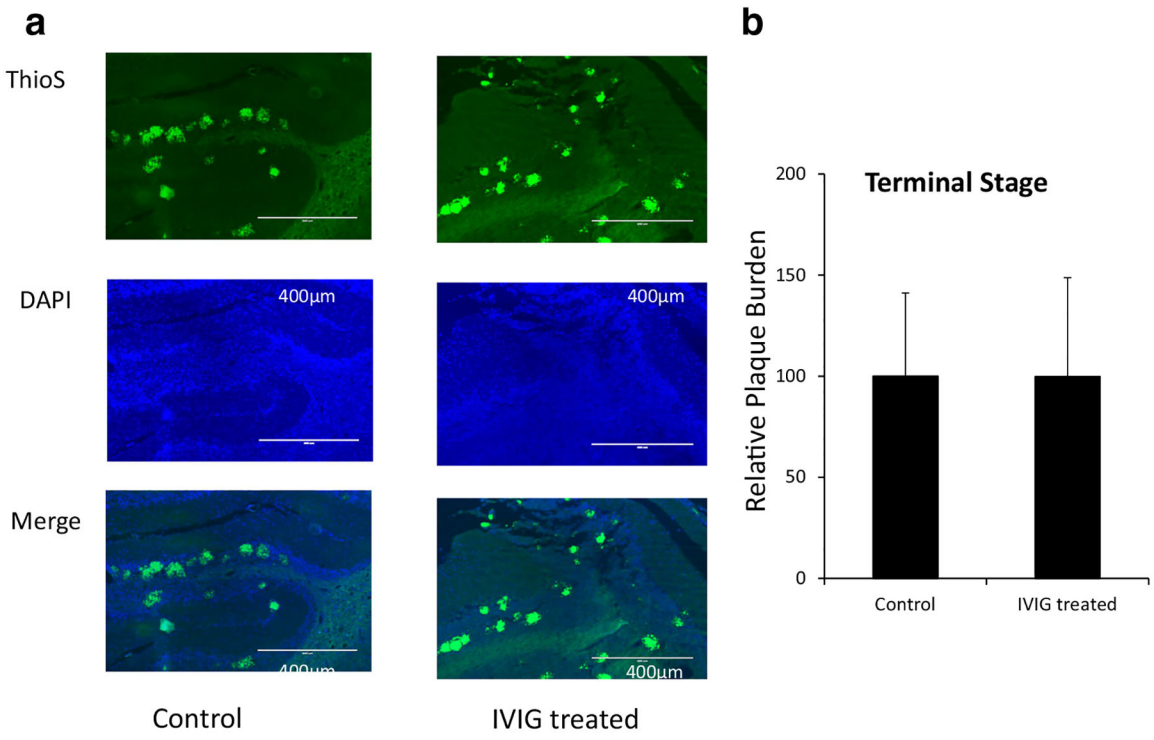

Fig. 4.

IVIG affects PrP amyloid plaque deposition in Tg (PrP-A116V) mice at terminal stage. **a** Representative cerebellum sections from Tg (PrP-A116V) mice (terminal stage) treated with PBS or IVIG. Sections were stained with thioflavin S to detect PrP amyloid plaques. Nuclei were stained with DAPI. Sections were visualized by fluorescence microscopy. **b** The area of thioflavin S staining was determined using ImageJ and plotted as the relative plaque burden. Data represent mean ± SD, $n = 3$/group, $^{*}p < 0.05$

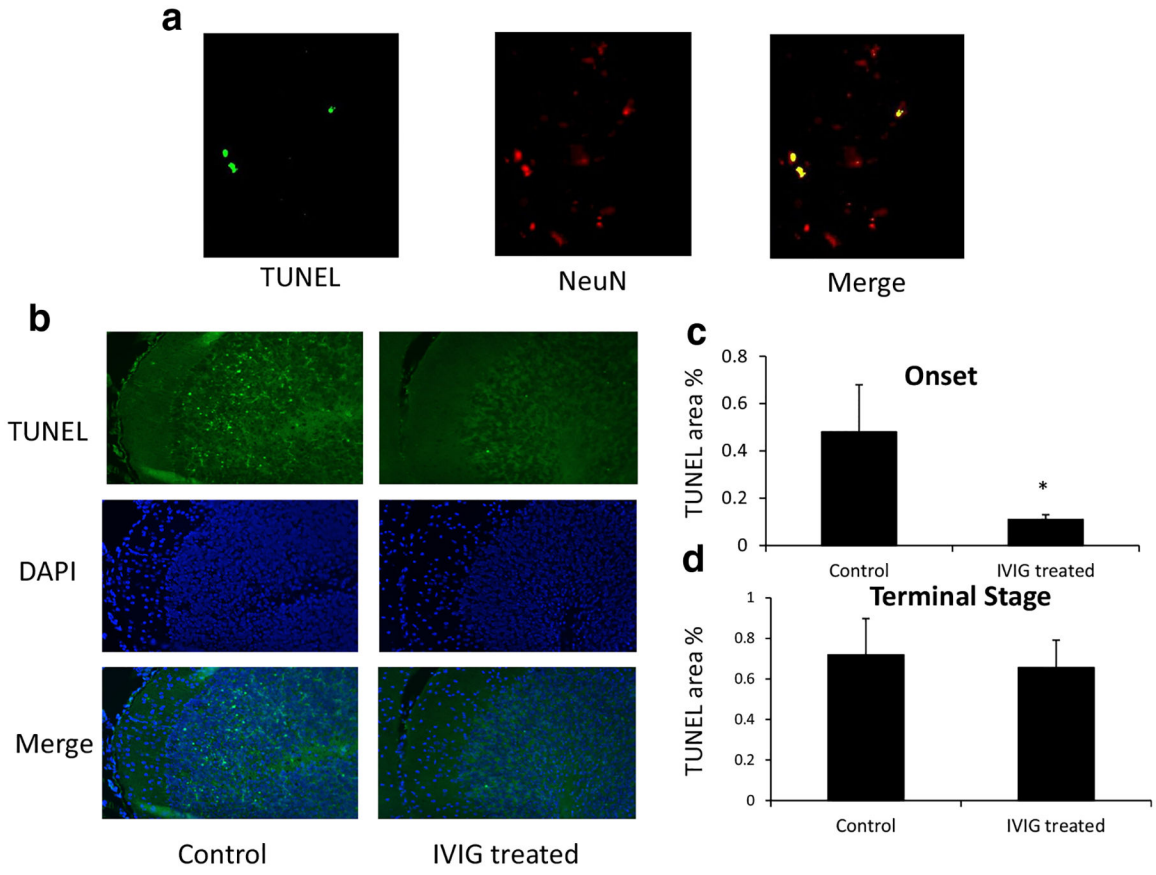

Fig. 5.

IVIG affects apoptosis in Tg (PrP-A116V) mice. TUNEL (green) and DAPI staining of representative cerebellum sections from 120 days old and terminal stage Tg (PrP-A116V) mice treated with PBS or IVIG. **a** Representative cerebellum sections from 120 days Tg (PrP-A116V) mice treated with PBS or IVIG. Apoptosis cells were estimated as the TUNEL-positive signal (green) was associated within NeuN-positive neurons (red). **b** TUNEL-positive nuclei (green) relative to the signal of DAPI-stained nuclei within each cerebellar section. **c** The fraction of apoptosis cells from 120 days mice. **d** The fraction of apoptosis cells from terminal stage mice. Data represent mean ± SD, $n = 3$/group, $*p < 0.05$

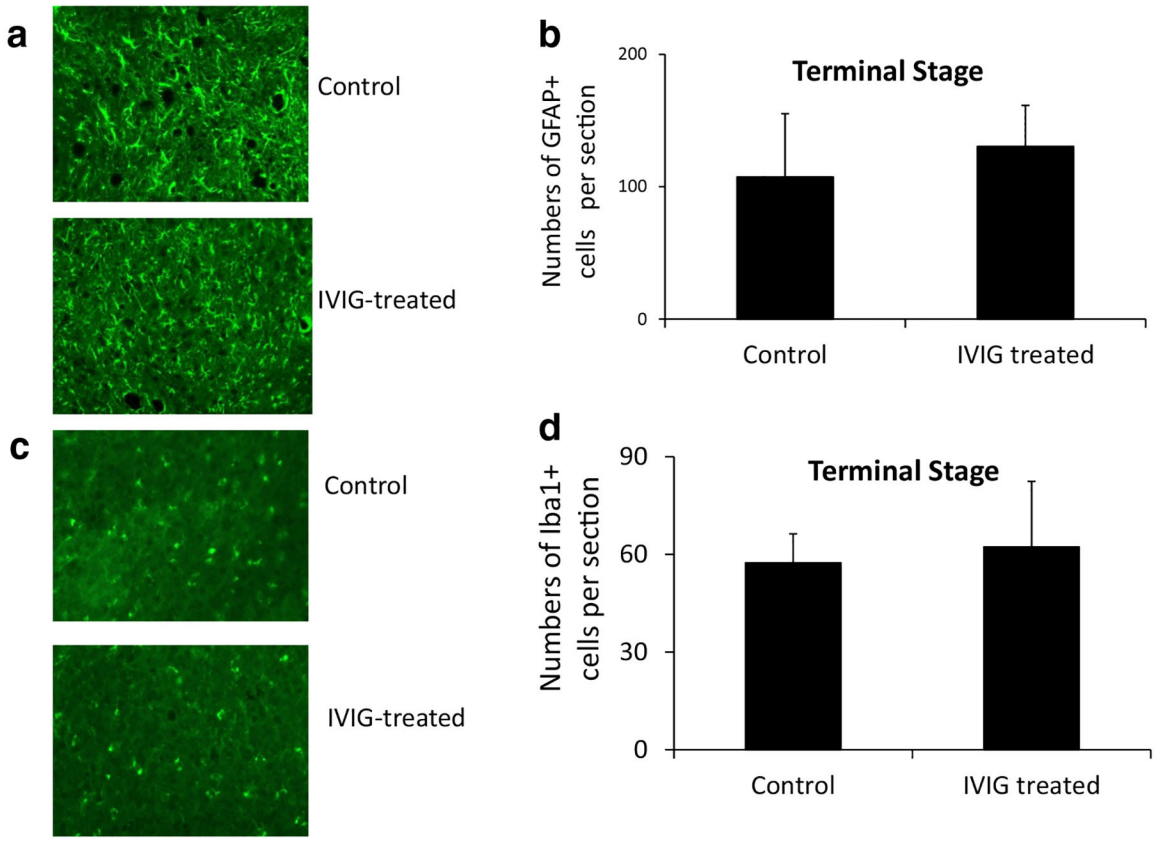

Fig. 6.

IVIG does not affect astrocyte and microglial activation in Tg (PrP-A116V) mice. Mouse anti-GFAP and anti-Iba1 antibody staining of cerebellar sections from terminal stage Tg (PrP-A116V) mice treated with PBS or IVIG. **a** Representative GFAP-stained cerebellum sections from terminal stage mice treated with PBS or IVIG. **b** Numbers of $GFAP^+$ cells from terminal stage mice. **c** Representative Iba1 cerebellum sections from terminal stage mice treated with PBS or IVIG. **d** Numbers of $Iba1^+$ cells from terminal stage mice. Data represent mean ± SD, $n = 3$/group